

EXAMINATION OF LATERAL DEVIATION OF A PROJECTILE SUBJECTED TO INTERNAL GYROSCOPIC FORCES

Christopher M. Umstead
Hamid M. Lankarani

Mechanical Engineering Department
Wichita State University
Wichita, Kansas, 67260-0133
USA

Abstract

The need for lateral travel can arise in a simple projectile either due to the target moving or to a transverse external force that moves the projectile. By the use of internal moving parts, a force in the lateral direction can be created, thus changing the flight trajectory of the projectile. Therefore, the possibility of the use of an internal gyroscopic force derived from a rotating disk could be used to counteract such activity. In this study, three internal swing masses attached at the end of a massless rod are located on the points of an equilateral triangle centered about the major axis of the projectile. The rotation of mass generates a normal acceleration and a subsequent force and torque upon the projectile. The force from combined movements of the masses can be used, to a small degree, to control the movement of the projectile. In this study, a model for this movement is derived mathematically and simulated on the computer using a developed code. For the cases examined, the projectile moves cyclically about the axis or deviated with a relatively even slope away from the axis. With these models, a parametric study is conducted with predetermined changes. The parametric study is focused on actuating each mass in sequence or changing the initial weight of the mass and starting position in relation to the projectile. A computer program is created in MATLAB for the developed model and the equations of motion are generated and solved numerically to simulate the flight of the projectile. The results from the simulation for the project are compared for differences in the projectile physical conditions. The results of this study show that the projectile could move in a lateral direction in a controlled manner. But the overall movement is minimal when compared to the size of the projectile or the distance traveled. While this application may not be suited for use in small projectiles, it may hold merit for use with larger craft or re-entry vehicles.

KEYWORDS: Projectiles, Flight trajectory, Gyroscopic effect, Mechanical system, Dynamics simulation

NOMENCLATURE

a	Scalar acceleration
\vec{a}	Acceleration vector
\vec{a}_d	Acceleration of the disk relative to the world
\vec{a}_p	Acceleration vector of projectile relative to the world
c_v	Viscous damping
F	Scalar force
\vec{F}	Acceleration vector
\vec{F}_{mass}	Force due to the rotating mass (sub-notation indicates which one)
I	Moment of inertia
m	Total mass of projectile
m_d	Mass of rotating weight (sub-notation indicates which one)
m_p	Mass of projectile minus moving parts
m_t	Mass of translating Weight
p	Point of rotation of the mass (sub-notation indicates which one)
r	Radius of rotating masses' arm relative to the projectile (sub-notation indicates which one)
\vec{r}	Radius vector of rotating masses' arm relative to the projectile (sub-notation indicates which one)
\vec{r}_p	Radius vector of the projectile relative to the world's origin

R	Radius of the projectile
rpm	Rotations per minute
v	Scalar velocity
\vec{v}	Velocity vector
α	Scalar angular acceleration
$\vec{\alpha}$	Angular acceleration vector
$\vec{\alpha}_d$	Vector angular acceleration of the mass relative to the world
$\vec{\alpha}_p$	Vector angular acceleration of the projectile relative to the world
τ	Scalar torque
$\vec{\tau}$	Torque vector
ω	Scalar angular Velocity
$\vec{\omega}$	Vector angular velocity

All units are presumed to be in the metric system unless noted.

1. INTRODUCTION

From medieval times with trebuchets destroying castles to launching modern satellite into orbit, the study of ballistics has been conducted to improve the flight course and end results. Early studies of control were done by means of changing the initial physical conditions. As technology developed, more study and research has been conducted in active control of the projectile during flight. The direct idea for control of the flight of a simple bullet in the lateral direction emerges from personal experience of watching bullets err from the desired target due to the influence of the wind. This idea of a single internal rotating mass is explored by Frost and Costello [1]. Several other researchers have explored different means of controlling and calculating trajectory. Control of a missile can be accomplished externally by fins and engines in flight. Internally, a projectile can be controlled by translating and rotating masses. The idea of a translating mass is that a weight is contained in a linear cavity within the projectile. The mass then slides within the cavity, creating a change of the center of gravity and conversely the angle of attack. Another version of the translating mass concept is attaching the mass to a rod of constant length which then rotates about the major axis of the projectile [2]. With the use of several of these rods, the center of gravity can be changed, and thus also changing the angle of attack.

The concept of a translating mass was explored by several investigators. According to Rogers and Costello [3], the trajectory changes due to a moving mass from the dynamic coupling between the two bodies. The equation that was found for the force acting from the translating mass in Equation (1) was converted from the frequency domain to the time domain [3]. When the mass was oscillated for a finned missile, the missile deviated in the lateral direction.

$$F_{Input} = \left(\frac{m_p m_t}{m} - m_t \right) a + (c_v - 2m_t \omega_n) v + m_t \omega_n^2 \quad (1)$$

The mass in this parametric study was offset from the center of gravity in a slot perpendicular to the major axis and oscillated. As was expected, an increase was found in the swerve as the mass moved away from the center of gravity. It was found as the slot moved away from the center of gravity, the control authority increased proportionally. If the slot is perpendicular to the major axis, the control of the missile is increased during the flight [4]. This is due to fact that the stability of the missile during launch can be increase, therefore reducing launch perturbations. Yet, when the missile is in flight, the stability can be reduced, giving greater control of the path of the missile. This effect indicates that as the missile with translating mass reaches the target, as opposed to a conventional missile just shy of reaching the target.

Changing the center of gravity by slowly rotating weights affixed about the major axis changed the angle of attack and conversely the flight path, was studied by Byrne [2]. He observed that while a minimum of two weights could be used, three or more weights require less drastic movement [2]. The base equation for the resultant center of mass in the polar coordinates was derived to Equation (2), and converted to Cartesian coordinate in Equation (3).

$$R_{eq} e^{i\theta_{eq}} = \frac{R}{3} (e^{i\theta_1} + e^{i\theta_2} + e^{i\theta_3}) \quad (2)$$

$$R_{eq} \begin{bmatrix} \cos \theta_{eq} \\ \sin \theta_{eq} \end{bmatrix} = \frac{R}{3} \begin{bmatrix} \cos \theta_1 + \cos \theta_2 + \cos \theta_3 \\ \sin \theta_1 + \sin \theta_2 + \sin \theta_3 \end{bmatrix} \quad (3)$$

The application of the translating mass is explored for possible use for reentry from orbit. In these figures, as the vehicle descended, the internal moving masses changed the direction of flight and directed the vehicle to the desired point of impact.

The notion of a single internal rotating disk was considered by Frost and Costello in several of their studies [1,5]. They found that, as the offset of the mass from the center of gravity increased, so also did the control. The equation of motion for the disk was found in Equation (4) and for the projectile body in Equation (5). Combining these together gives Equation (6), which is the equation of motion for both the projectile and the rotating disk.

$$m_d \vec{a}_d = \vec{F}_R + \vec{W}_d \quad (4)$$

$$m_p \vec{a}_p = -\vec{F}_R + \vec{W}_p + \vec{F}_A \quad (5)$$

$$m_p \vec{a}_p + m_d \vec{a}_d = \vec{W}_{dD} + \vec{W}_p + \vec{F}_A \quad (6)$$

From these equations, a control system for the projectile can be developed. The movement in the lateral direction was demonstrated with the two body systems containing the rotating disk. This concept of a single rotating disk is expanded in the current study in a parametric study of three rotating disks, and the effect of the rotation on the lateral movement of the projectile is investigated.

The objective of this current study is thus to conduct a parametric study on the concept of controlling a projectile by the controlled spinning of one to three internal masses. The masses are mounted atop mass-less rods. These rods are then pinned on the opposite end to the main body of the projectile, equally distanced from each other and the major axis of the projectile. In the parametric study, the mass, the starting orientation, and the angular rotation of the disks are systematically varied, and the results are examined and compared with one another. From these results, recommendations for possible further studies and improvement are given.

2. METHODOLOGY

In this study, mathematical models of different projectiles are developed and their corresponding equations of motion are derived and solved numerically using the MATLAB computer program. A base solid core projectile model is first examined, after which a concept projectile model with three rotating weights is investigated. The entire concept projectile system will have nine degrees-of-freedom, six for the projectile and one for each rotating disk. Controllable inputs into the model are initial linear and angular velocity and acceleration of the projectile and disk. After the projectile is in flight, control will be established by the changing rotational velocity of the disks, which will in turn change the course of flight. Other force beyond direct control and acting upon the projectile during flight beyond direct control will be drag and gravity.

2.1 Physical Projectile Properties

The model analyzed is of a projectile 20 mm in diameter. The shape of the projectile is a simple cone shape for the head attached to a cylinder. Figure 1 shows the sketch and computer model of the projectile; the major axis is equivalent to the x-axis of the system in all subsequent references. The mass of the model considered is between 130 gm and 400 gm depending on conditions. The results from the following study, however, can be sequentially scaled up for larger models because equations of motion are linear with respect to masses, rod lengths for the rotating mass, and linear velocity. The nonlinear part of the equation of motion is the angular velocity of the mass, which has an exponential effect, and the angle of the mass rod which changes trigonometrically.

2.2 Solid Core Projectile Model

The traditional model is a projectile of a solid core with no moving parts. It is assumed the greatest force acting upon it during its flight is gravity and the path will be parabolic due to the acceleration. The environment considered is a simple world of six-degrees-of-freedom. Studies have been conducted on predicting the flight path of a projectile and simplifying the equations to linear forms [5,6].

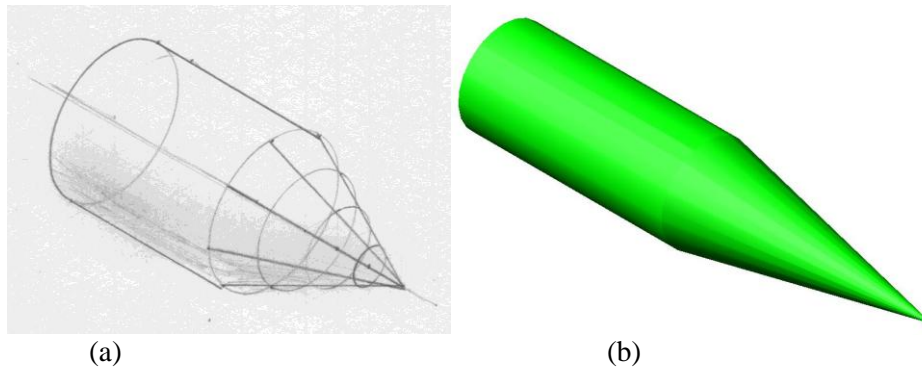


Figure 1. Solid CoreProjectile:

(a) Sketch of the Projectile,

(b) Computer Model of the Projectile.

The bases of the mathematic model is the Newton’s first law, $\vec{F} = m\vec{a}$. The components of \vec{F} in this case are gravity and force induced from flight, the largest of which, in this case, is drag. For the simple projectile, \vec{F} is equal to the sum of the drag forces, which is given in equation (7), and gravity, which is acting in the direction, given in Equation(8), where ρ is the density of the air; C_d is the drag coefficient; A is the cross sectional area; and θ is the angle of the major axis relative to direction of gravity.

$$\vec{F}_{drag} = -\frac{1}{2}\rho|\vec{v}|^2C_dA\vec{v} \tag{7}$$

$$\vec{F}_{gravity} = \begin{bmatrix} 0 \\ \sin \theta g \\ \cos \theta g \end{bmatrix} \tag{8}$$

Combining these forces in the equation of motion, Equation (9) is derived and gives the basic parabolic arc for a projectile.

$$\vec{F}_{drag} + \vec{F}_{gravity} = m\vec{a} \tag{9}$$

For verification, the dynamics of the solid core projectile model was first simulated using the MATLAB program developed. The construction of the model was a cylinder with a cone mated to the top. The model is initially at point zero with the bottom of the cylinder located thus and the major axis passing through the point. Because all forces are acting through the center of gravity, torque will not be induced or need to be accounted for. The gravity force vector was angled to simulate a 15-degree tilt and initial velocity was set to 800 m/s. The flight of the projectile performed as expected with the projectile traveling in a parabolic arc, as shown in Figure 2.

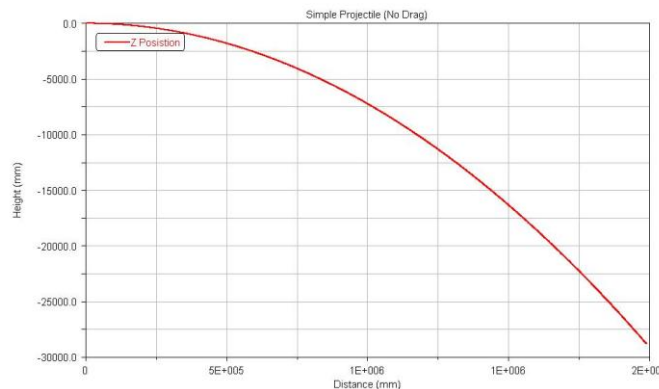


Figure 2. Solid Core Projectile Flight of Elevation versus Distance Traveled.

2.3 Concept Projectile Model

The concept of the new model, as shown in Figure 3, is to incorporate three weights that could be rotated about a point within the projectile and cause a deviation in the flight path, specifically in the lateral direction. The rotation points are the tips of an equilateral triangle centered about the major axis of the projectile, as shown in the figure.

Letting r be the maximum length of the rotation mass such that $2r$ is one of the legs of the equilateral triangle. Then the position of the rotation points are $(0, \frac{2\sqrt{3}}{3}r)$, $(-r, -\frac{\sqrt{3}}{3}r)$, and $(r, -\frac{\sqrt{3}}{3}r)$ respectively, with the origin located in the center of the triangle. The minimum radius for the projectile, R , in terms of r , is shown in Equation(10).

$$R = \left(\frac{2\sqrt{3}}{3} + 1\right)r \approx 2.155r \tag{10}$$

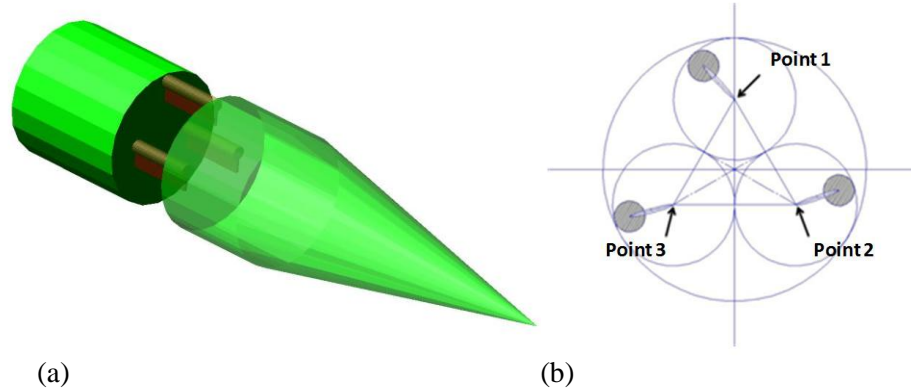


Figure 3. Concept Projectile:
(a) CAD Projectile Model,

(b) Cross Section Rotation Points.

The idea is when the masses are rotated the gyroscopic force generated will cause the projectile to deviate. By the use of three masses, the direction of the deflection can be controlled in the lateral direction. The model for this system is composed of three rotating masses represented as cylinders connected to mass-less rods which rotated about a point. The three rotation points were located at the peaks of an equilateral triangle with the center of the triangle coinciding with the major axis of the projectile. The parameters for design were segment lengths, masses of each part, and the initial starting angular and linear velocities. By the use of parameters, it was possible for the model to be quickly changed to simulate the scenario changes. The changes made to the model were the variations of initial angular velocities, mass ratios, and phases of the weights' positions to analyze the effect of the change down-range in the lateral direction.

The equation for motion of the projectile was derived from equations from several studies and modified for this study [1,6,7]. Combining Equations (7) and (8) with Equation (11) for each mass gives Equation (12), which gives the overall force equation for the system. Thus, the overall encompassing equations for force is

$$\vec{F}_{mass} = m_d(\vec{a}_p + \vec{\alpha}_p \times \vec{r}_p + \vec{\omega}_p \times (\vec{\omega}_p \times \vec{r}_p) + \vec{\alpha}_d \times \vec{r}_{CD} + \vec{\omega}_d \times (\vec{\omega}_d \times \vec{r})) \tag{11}$$

$$m_p(\vec{a}_p + \vec{\omega}_p \times \vec{v}_p) + \sum_{i=1}^n (m_{d_i}(\vec{a}_p + \vec{\alpha}_p \times \vec{r}_{PC,i} + \vec{\omega}_p \times (\vec{\omega}_p \times \vec{r}_{p,i}) + \vec{\alpha}_{d,i} \times \vec{r}_i + \vec{\omega}_{d,i} \times (\vec{\omega}_{d,i} \times \vec{r}_i)) = \left(m_p + \sum_{i=1}^n m_{d_i}\right) * \vec{g} - \frac{1}{8} * C_d * \rho * \left|\vec{v}_p\right|^2 \pi d^2 \vec{v} \tag{12}$$

Torque is created by the offset of the rotation point from the major axis, with the resulting force from the normal acceleration upon that point as given in Equation (11). Using $\vec{\tau} = I\vec{\alpha}$, the angular acceleration of the projectile can be found, and conversely the angular velocity of the project can be found [8]. This rotation of the projectile changes the angle of the rod of the rotating disk and the location of the point of rotation with respect to the ground and subsequently the direction of force that is created by the disk on the projectile.

$$\vec{\tau} = \sum_{i=1}^3 \vec{p} \times \vec{F}_{mass_i} \tag{13}$$

The polar moment of inertia about the major axis was estimated by treating the main body of the projectile like a solid cylinder and the masses as points, giving Equation (14). With the moment of inertia and torque, the angular velocity of the projectile was found along with the subsequent changes in the location of rotation points and arms.

$$I = \frac{1}{2} m_p R^2 + \sum_{i=1}^3 m_d |\vec{r}_i + p_i|^2 \quad (14)$$

Using the equations discussed above, a simulation program was created in MATLAB to find velocity and position, both linear and angular, of the projectile and the disk. This was primarily accomplished by breaking Equations (11) and (12) into sub-equations and solving for the parts for ease and cleanness of code. The dynamics equations of motion were numerically solved using the Euler method with a given step-size and checking the accuracy of the method with Richardson error estimate. The Runge-Kutta fourth-order with fifth-order correction (ode45 in MATLAB) with adjustable step-size was also utilized for further checking the accuracy of the numerical solutions obtained. The structure of the program was loops within loops. For each major loop, one of the initial starting conditions was changed. These variables were the disk mass, initial phase, and initial angular velocity. The results of position and velocity of the disks and projectile would then be stored in a file for later recall to be analyzed either manually or by a sub-program.

3. RESULTS FROM CONCEPT MODEL PARAMETRIC STUDY

The model was subjected to a series of parametric changes to determine what parameters induced the greatest deviations of the projectile in the lateral directions. The concept is if a deviation can be induced to change the flight path from the spinning weight; then conversely, the same force can be used to correct for an external random force upon the projectile. Therefore, the deviation of the path of the projectile in the lateral direction was observed compared. The parametric study change occurred in the order presented in Figure 4. First, the phase or initial position of the mass was set according to the parameter being examined. The mass was then either changed to one of three possible weights or remained the same while the angular velocity possibilities were cycled. The angular velocity of the masses were changed to reflect a given scenario represented by ωN , where N is a letter between A and F designating what conditions are occurring, as seen in the following tables. The results from these changes are recorded in spreadsheet form. The results are plotted and then compared.

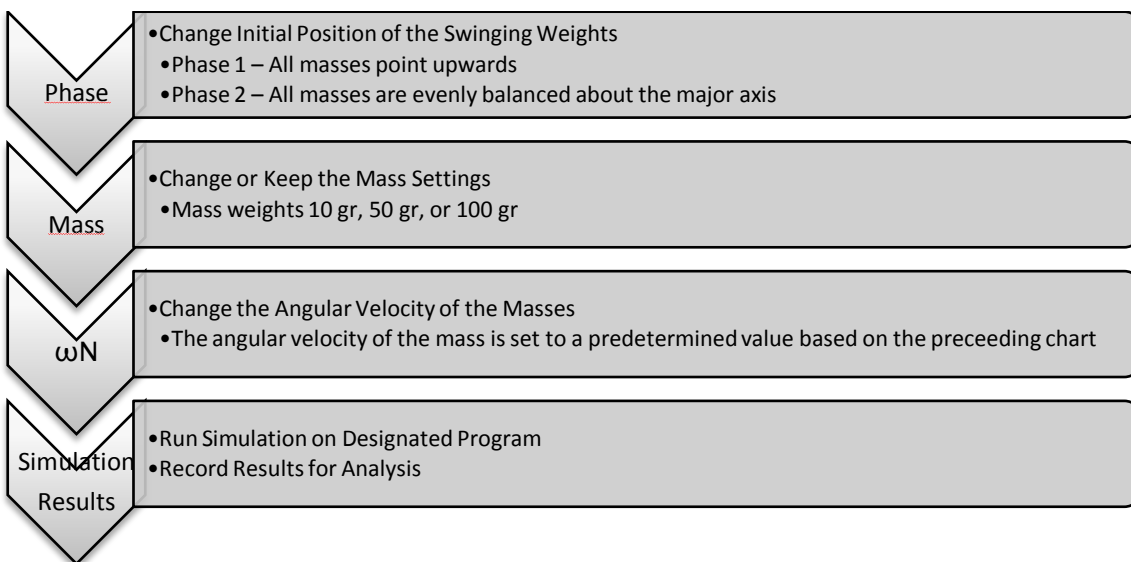
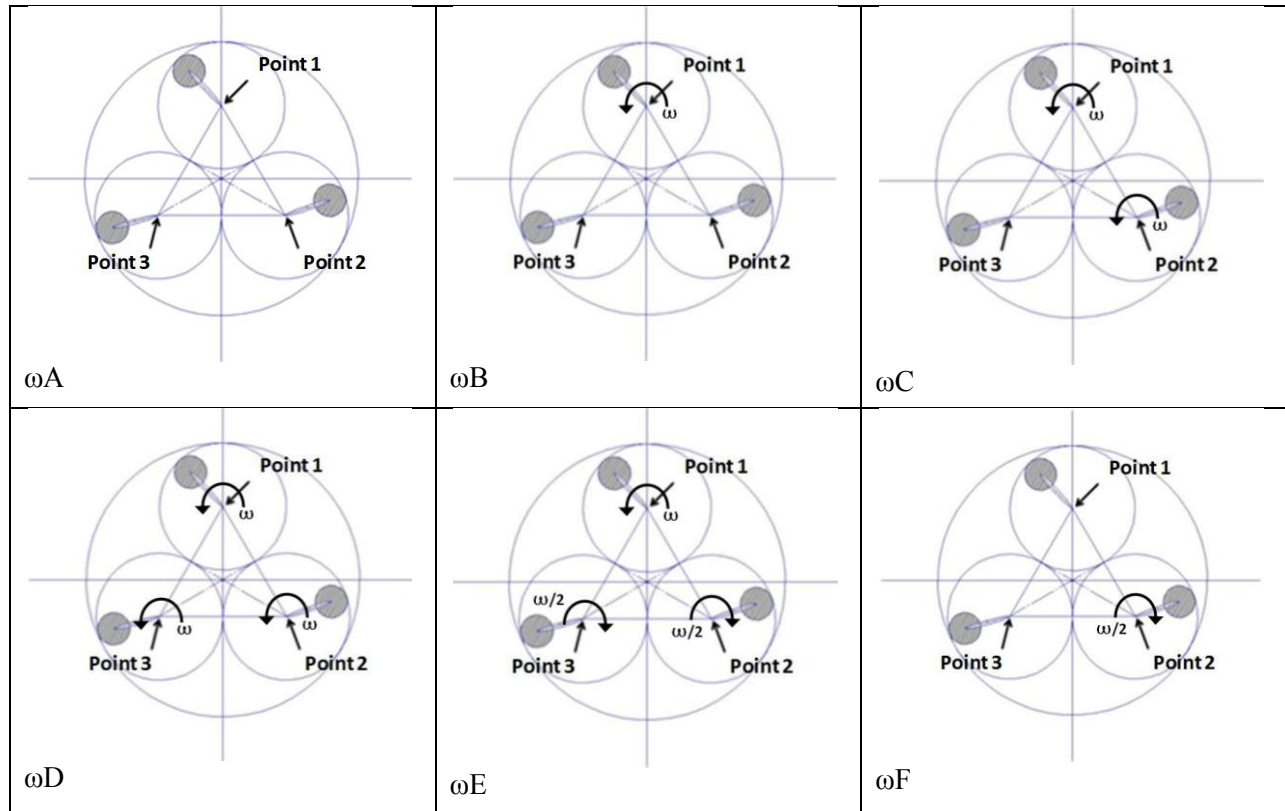


Figure 4. Parametric Study Flow Chart.

Table 1. ω Conditions and Diagrams.



3.1 Parametric ω Change Study

As stated, the angular velocities of the masses were changed to one of six conditions designated by a letter. In Table 1, the order of what masses are rotated for a given conditions is shown. The first case, ωA , all the masses are held at a standstill and there is no deviation lateral of the projectile. In ωB , the top mass is rotated at a constant velocity relative to the projectile. This rotation causes the projectile to both rotate and move because of the induced force. In cases ωC and ωD , the other two masses are spun sequentially. In the next case, ωE , the two lower masses are spun at half the velocity of the upper mass and in the opposite direction. In ωF , mass 3 is at half the angular velocity of ωB and in the opposite direction.

3.2 Parametric Weight Change Study

The weight of the masses was changed a total of four times, as shown in Tables 2, 3, and 4, with the other parameters changing for simulations to be compared. The mass of the non-moving part of the projectile was held at 100 grams equally distributed about the center of mass. The lowest ratio of weight of the rotating masses to overall weight is 0.23 and the largest is 0.75.

Table 2. Mass Conditions 1.

ω Condition	ω_1 (rpm)	ω_2 (rpm)	ω_3 (rpm)
ωA	0	0	0
ωB	167	0	0
ωC	167	167	0
ωD	167	167	167
ωE	167	-83.3	-83.3
ωF	0	0	-83.3
$\theta_1 = \theta_2 = \theta_3 = 90^\circ$			
$m_{d,1} = m_{d,2} = m_{d,3} = 10\text{ gr}$			

Table 3. Mass Conditions 2.

ω Condition	ω_1 (rpm)	ω_2 (rpm)	ω_3 (rpm)
ω_A	0	0	0
ω_B	167	0	0
ω_C	167	167	0
ω_D	167	167	167
ω_E	167	-83.3	-83.3
ω_F	0	0	-83.3
$\theta_1 = \theta_2 = \theta_3 = 90^\circ$			
$m_{d,1} = m_{d,2} = m_{d,3} = 50 \text{ gr}$			

Table 4. Mass Conditions 3.

ω Condition	ω_1 (rpm)	ω_2 (rpm)	ω_3 (rpm)
ω_A	0	0	0
ω_B	167	0	0
ω_C	167	167	0
ω_D	167	167	167
ω_E	167	-83.3	-83.3
ω_F	0	0	-83.3
$\theta_1 = \theta_2 = \theta_3 = 90^\circ$			
$m_{d,1} = m_{d,2} = m_{d,3} = 100 \text{ gr}$			

The MATLAB code for the model was then created with the form of the program loops embedded within each other to change the conditions sequentially. The rotation masses were set to 0.010 kg and spun with angular velocity as specified in Table 2. The results of this simulation are shown in Figure 5 with each color line representing a different omega condition as laid out in the table. The greatest deviation for this case occurred for ω_D condition, with a total deflection of 39 mm.

The extra weight caused the projectile to deflect more in Weight Condition 2 than in Weight Condition 1 as expected. Also, the greatest deflection occurred when all the masses rotated in the same direction with the same angular velocity. The results for all these simulations are shown in Figure 6 with each ω condition, as specified in Table 3. A deviation of 101 mm; this deviation was the greatest deviation out of all the masses cases examined for this phase.

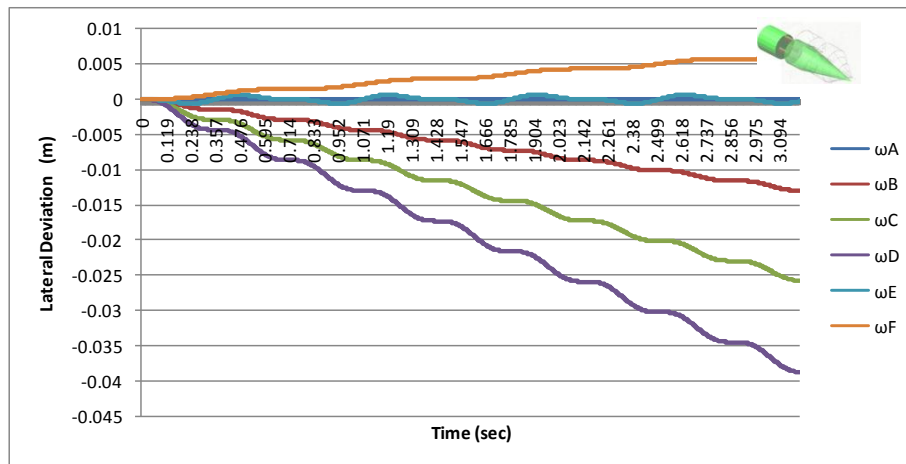


Figure 5. Lateral Deviation of the Concept Projectile for Mass Condition 1 and All ω Conditions.

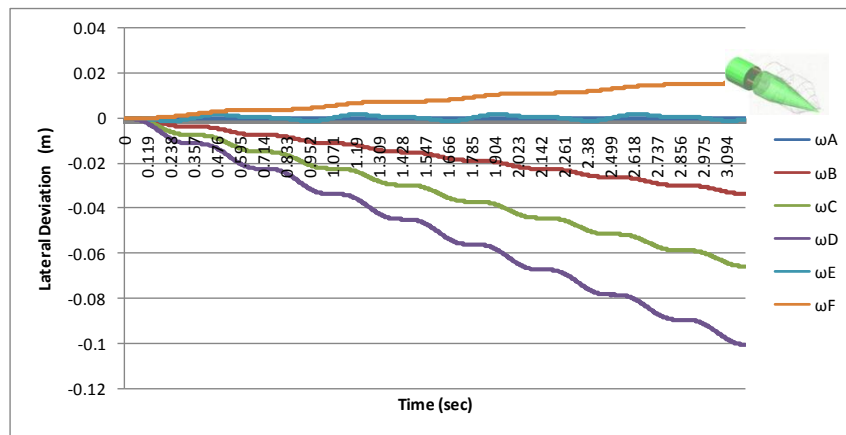


Figure 6. Lateral Deviation of the Concept Projectile for Mass Condition 2 and All ω Conditions.

In Weight Condition 3, the greatest deviation for most cases of the weight conditions occurred when all the angular velocities are the same, similar to the other cases, as seen in Figure 7. The maximum deviation for this case, and all the computer simulation cases, was 82mm.

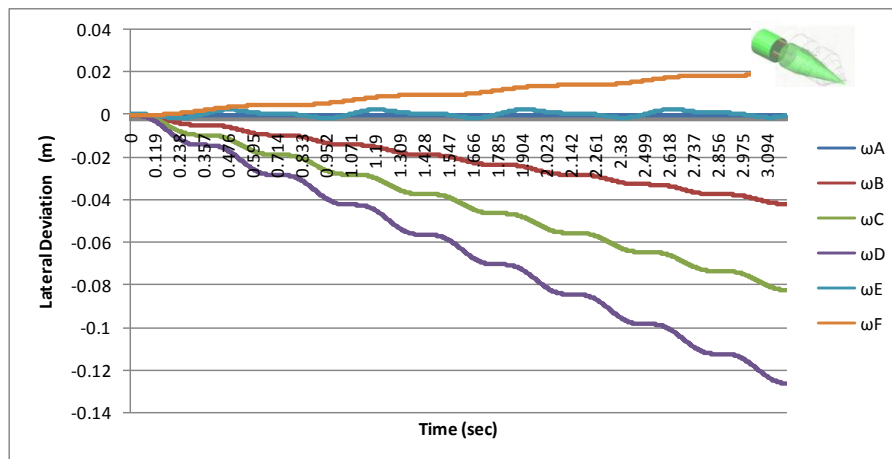


Figure 7. Lateral deviation of the concept projectile for Mass Condition 3 and All ω Conditions.

3.3 Parametric Phase Change Study

The phase in this study is specified as the location of the rotating masses with respect minor axes. The initial phase of the mass was changed by rotating the mass from the starting position, as shown in Figure 8, to an evenly-balance position about the major axis, as shown in Figure 9. The position of the masses corresponds to Tables 5 and 6 respectively. Each of the phase changes was subjected to similar parametric studies as to weight changes, and corresponding results are shown in Figure 10. It was found that if all the initial angular velocities of the mass were the same for all three masses, as stated for ω_D , the movement of the projectile would be cyclic with the mean being a negated movement.

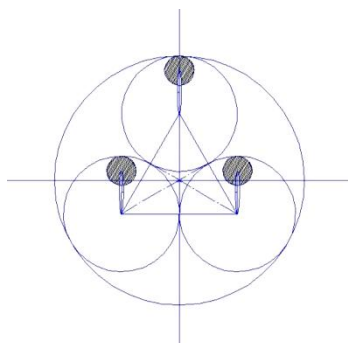


Figure 8. All Masses at 90 Degrees as Specified in Phase Condition 1.

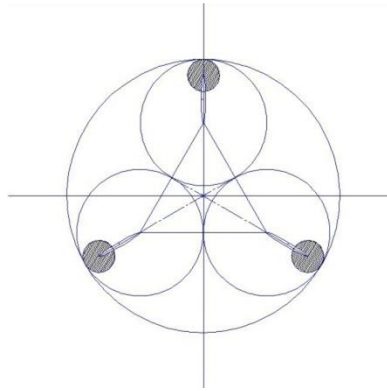


Figure 9. Masses in Equilateral Triangle as Specified in Phase Condition 2.

Table 5. ω and Phase Condition 1.

ω Condition	ω_1 (rpm)	ω_2 (rpm)	ω_3 (rpm)
ω_A	0	0	0
ω_B	167	0	0
ω_C	167	167	0
ω_D	167	167	167
ω_E	167	-83.3	-83.3
ω_F	0	0	-83.3
$\theta_1 = \theta_2 = \theta_3 = 90^\circ$			
$m_{d,1} = m_{d,2} = m_{d,3} = 10mg$			

Table 6. ω and Phase Condition 2.

ω Condition	ω_1 (rpm)	ω_2 (rpm)	ω_3 (rpm)
ω_A	0	0	0
ω_B	167	0	0
ω_C	167	167	0
ω_D	167	167	167
ω_E	167	-83.3	-83.3
ω_F	0	0	-83.3
$\theta_1 = 90, \theta_2 = 210, \theta_3 = 330^\circ$			
$m_{d,1} = m_{d,2} = m_{d,3} = 10mg$			

Using the same computer simulation program, the initial starting phase of the masses was changed according to the Tables 5 and 6. The results from Condition 1, as specified in Table 5, were exactly the same, produced the results as shown in Figure 5. The results from Phase Condition 2, as specified in Table 6, are shown in Figure 10. The greatest deviation occurred for ω_E , shown by the light blue line in Figure 10 with a total deviation of 19 mm. In the case of ω_D , the gyroscopic force was all but negated within the system, and the projectile path was along the center line with no deviation laterally.

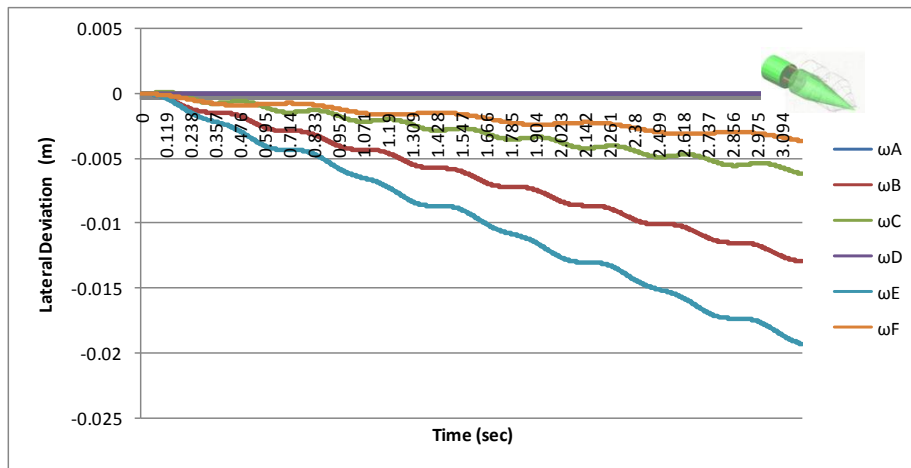


Figure 10. Lateral Deviation of the Concept Projectile for Mass Condition 1 Phase Condition 2.

3.4 Comparison of Reaction to Parametric Mass Change

The selected results of the deviation were overlaid with each other for comparison. The effect of the different masses used to calculate the deviation was then evaluated. The case for which the greatest deviation occurred varied from mass case. Phase 1, according to Table 5, was used for all initial phases for the Mass Conditions changes. According to the simulations, Mass Condition 2 had the greatest overall deviation for the Case ωD , as seen in Figure 7; this trend continued in all the other cases looked at where ωD had the greatest deviation. In case of ωB , ωC , and ωD the trend of the projectile was to have a negative slope regardless of what mass was being used. This can be seen in Figures 11 and 12, for each case respectively. In case of ωE , the masses swinging in the opposite direction of the upper mass had a net canceling effect, and the projectile merely alternated the direction of traveling, as shown in Figure 13, with a mean deviation of zero. In case of ωF the slope of the trajectory was positive, as seen in Figure 14, because of the one mass rotating in an opposite direction when compared to ωB .

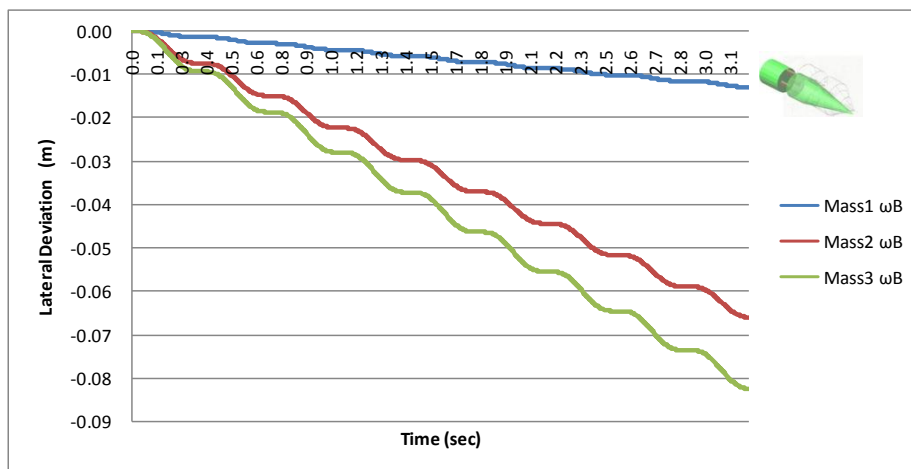


Figure 11. Lateral Deviation of Concept Projectile for Mass Comparison of ωB .

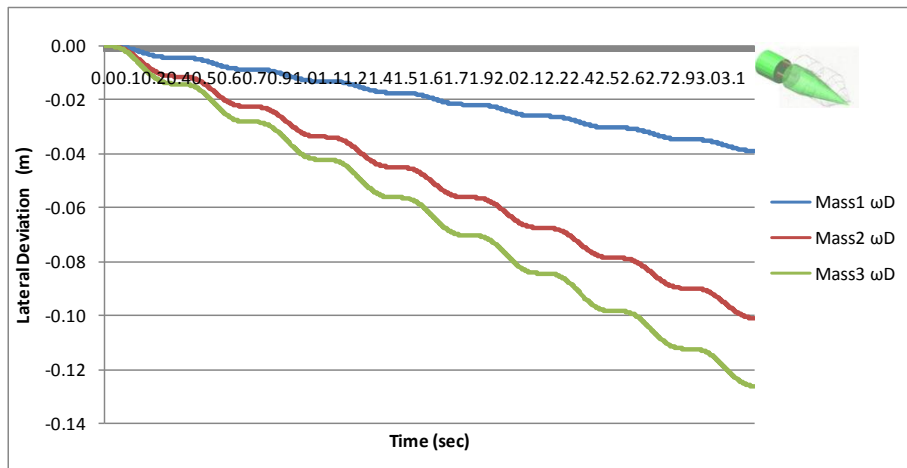


Figure 12. Lateral Deviation of the Concept Projectile for Mass Comparison of ωD .

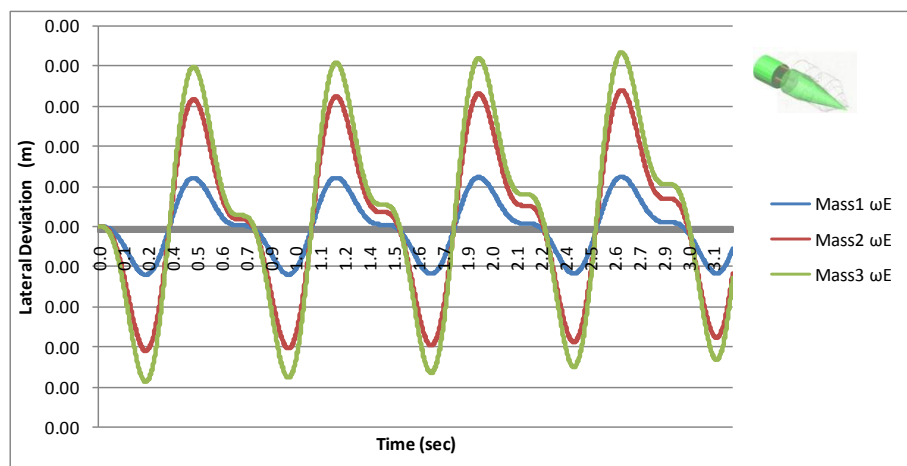


Figure 13. Lateral displacement of concept projectile for Mass Comparison of ωE .

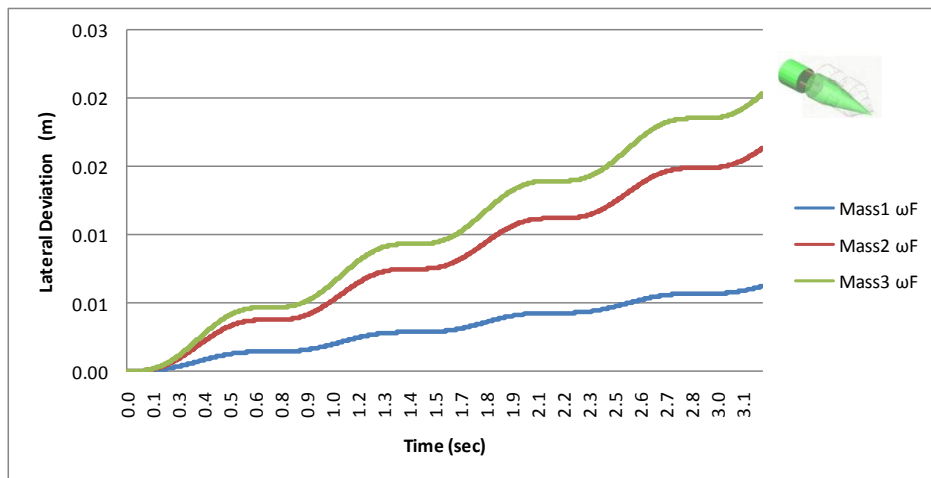


Figure 14. Lateral Deviation of Concept Projectile for Mass Comparison of ωF .

3.5 Comparison of Reaction to Parametric Phase Change

The selected results of the deviation were overlaid with each other for comparison. The effect of the different starting phase (either all the masses were initially pointed upward or evenly balanced) used to calculate the deviation was then evaluated. The two cases of initial phase that were examined were when the rod masses were parallel to each other, as shown in Figure 8.

The other case was when all masses were equally spaced apart with the angle between the rods being 120 degrees, as shown in Figure 9. The case of Phase 1 among the different simulations has already been compared above. In all cases when Phase 1 is compared to Phase 2 for case ωB , the deviation of the projectile is identical as would be expected because it is the center mass which is in a vertical position for both cases. In the simulations, the difference in the deviation of the projectile depending on phases can be seen in Figure 15. The greatest difference in the action of the projectile took place for ωD and ωE , which is amplified in Figure 16. The projectile path behaved as expected in that, for Phase2, the projectile stayed along the axis for ωD and deviated for ωE . But for Phase1, it behaved in the opposite manner--deviating for ωD and traveling along the axis for ωE .

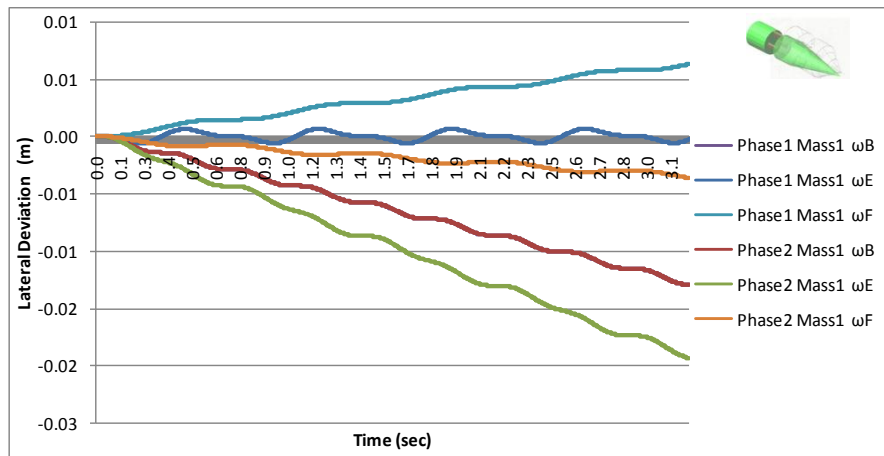


Figure 15. Lateral deviation of concept projectile for Phase 1 and 2 Comparison Mass1 of ωB and ωE .

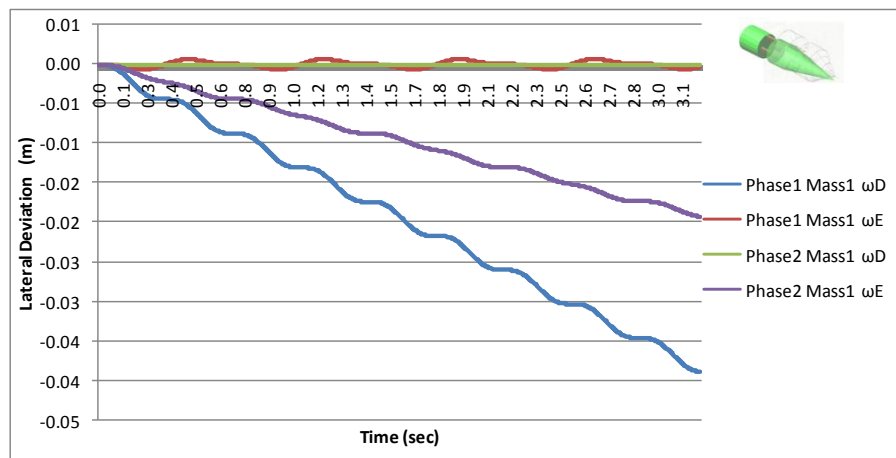


Figure 16. Lateral Deviation of the Concept Projectile for Phase 1 and 2 Comparison Mass 1 of ωD and ωE .

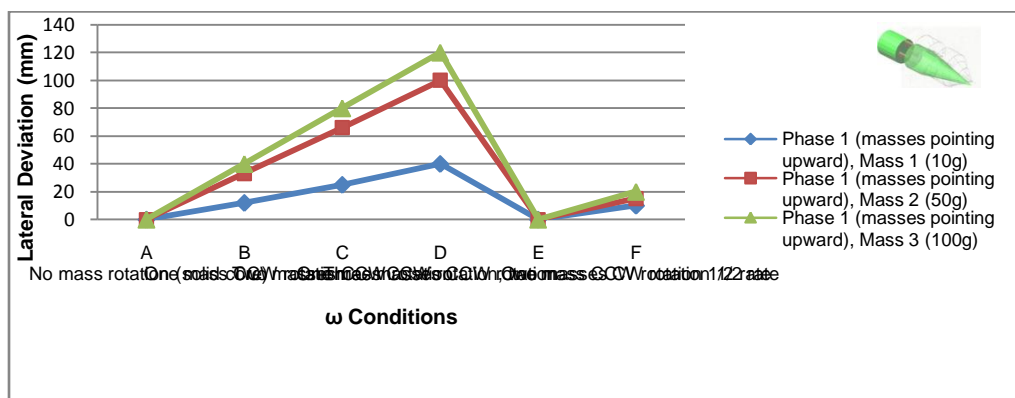


Figure 17. Maximum Deviation Comparison for all Mass Conditions, all ω Conditions, for Phase 1 (All masses pointing upward).

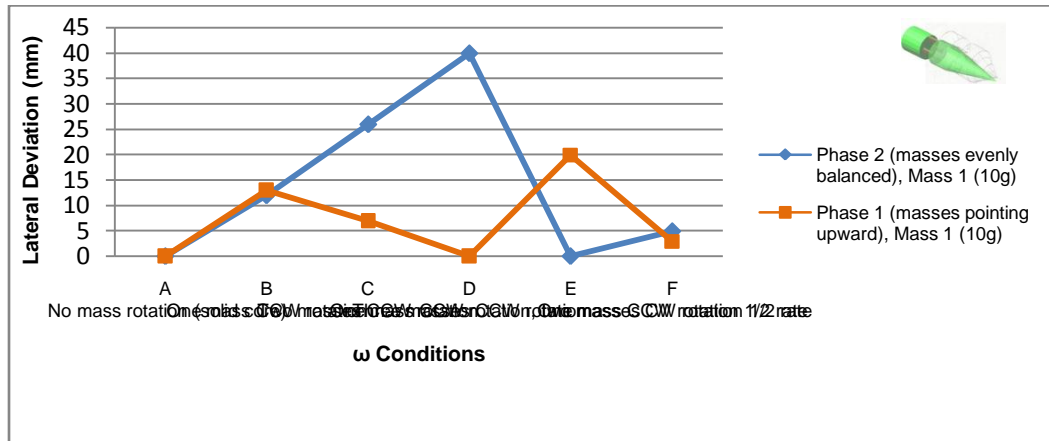


Figure 18. Maximum Deviation Comparison for Mass1, all ω Conditions, Phase 1 (all masses pointing upward) and 2 (masses evenly balanced).

4. CONCLUSION

This study was aimed at conducting a parametric study on the concept of controlling a projectile by the controlled spinning of one to three internal masses. The masses were mounted atop mass-less rods, and these rods were then pinned on the opposite end to the main body of the projectile, equally distanced from each other and the major axis of the projectile. The governing equations of motion of the projectile were generated and numerically solved. In the parametric study, the mass, starting orientation, and angular rotation of the disks were systematically changed, and the results were captured. Examination of the results from this study revealed that the projectile deviated from line of travel when it was subjected to an internally gyroscopic force. Because the deviation of the projectile can be controlled, the flight path could be corrected to counteract an undesired movement in the lateral direction. A summary of the results in terms of maximum deviation for the various configurations are shown in Figures 17 and 18. The deviation varied depending on the initial conditions, with the greatest deviation just over 100 mm in Mass Condition 2, Phase 1, for ω D (all three masses rotating with the same rate and in the same direction), as seen in Figure 6. Yet, considering the diameter of the projectile being considered, 20mm, the deviation was just over 5 times the diameter. With a continuous slope over a range of 2500 meters, the implementation of this system is probably not worth the effort or the expense. Also with the given slope of the deviation, it renders nearly impractical for arcing the projectile around an object in the flight path or correcting to external deviating forces.

To improve this system, one could devise a control system to do ‘real time’ correction for minor deviations. More research in the effect of the initial phase of the mass could be examined or orienting the position of the rotation axis to not parallel to the major axis of the projectile. Moving the orientation of the axis would have a similar effect, but initial speculation would anticipate a more chaotic flight path. The speculative development and production cost of design for one-use projectiles would most likely adversely outweigh any improved accuracy adversely. The funds and efforts could be put to better use in designing a more robust adaptive targeting system to consider initial conditions before launching the solid core round at the target. For far larger applications such as reentry vehicles the idea of rotating internal members may have use by adding stability or control to the system. This concept may pose merit, especially if already existing systems such as robot arms could be implemented and if it would merely be adding a control system to existing onboard computers.

Overall, the movement of the projectile behaved as expected with greatest deviation occurring for the case of ω D for the case of Phase 1, when all three masses were rotating at the same rate and in the same direction. Yet this movement was negated when the initial phase was changed to Phase 2. Also, for ω E for Phase 1, when one mass rotated in one direction and the other two at half rate in the opposite direction, the lateral deviation was minimal, as was anticipated. In general, the results from this study may have possible application for flight vehicles other than small simple projectiles.

5. REFERENCES

- [1] Frost, G., &Costello, M. (2003). "Stability and Control of a Projectile with an Internal Rotating Disk," AIAA Atmospheric Flight Mechanics Conference and Exhibit, Austin, Texas.
- [2] Byrne, R. H., Robinett, R. D., &Sturgis, B. R. (1996). "Moving Mass Trim Control System Design," AIAA, Guidance, Navigation and Control Conference, San Diego, California.
- [3] Rogers, J., &Costello, M. (2007). "Flight Dynamics and Control Authority of a Projectile Equipped with a Controllable Internal Translating Mass," AIAA Atmospheric Flight Mechanics Conference and Exhibit, Hilton Head, South Carolina.
- [4] Rogers, J. &Costello, M. (2008). "A Variable Stability Projectile Using an Internal Moving Mass," AIAA Atmospheric Flight Mechanics Conference and Exhibit, Honolulu, Hawaii.
- [5] Frost, G., &Costello, M. (2004). "Linear Theory of a Rotating Internal Part Projectile Configuration in Atmospheric Flight," *Journal of Guidance, Control, and Dynamics*, 27(5), 898-905.
- [6] Ollerenshaw, D., &Costello, M. (2008). "Simplified Projectile Swerve Solution for General Control Inputs," *Journal of Guidance, Control, and Dynamics*, 31(5), 1259-1265.
- [7] Hainz, L. C., &Costello, M. (2005). "Modified Projectile Linear Theory for Rapid Trajectory Prediction," *Journal of Guidance, Control, and Dynamics*, 28(5), 1006-1014.
- [8] Beer, F. P., Johnston, E. R., & Clausen, W. E. (2004). *Vector Mechanics for Engineers Dynamics*, (7th ed.). New York: McGraw Hill.